Baghdad Science Journal

Volume 23 | Issue 3 Article 19

3-23-2026

A Novel Graphene Nanoplatelets Electrochemical Aptamer Biosensor for Glycated Human Albumin Detections

Hadi Al-Sagur
Department of Physiology and Medical Physics, College of Medicine, University of Thi-Qar, Nasiriyah, Iraq AND Materials and Engineering Research Institute, Sheffield Hallam University, Sheffield, United Kingdom, hadi@utq.edu.iq

Ali Al-Jawdah
Department of Physics, College of Science, University of Babylon, Hilla, Iraq, aalimadlol@yahoo.com

Ali Al-Khazraji
General Directorate of Education in Salah Al-Din, Ministry of Education, Iraq, ali.chemistry86@gmail.com

Alexei Nabok
Materials and Engineering Research Institute, Sheffield Hallam University, Sheffield, United Kingdom, alexei.nabok@gmail.com

How to Cite this Article

Al-Sagur, Hadi; Al-Jawdah, Ali; Al-Khazraji, Ali; and Nabok, Alexei (2026) "A Novel Graphene Nanoplatelets Electrochemical Aptamer Biosensor for Glycated Human Albumin Detections," *Baghdad Science Journal*: Vol. 23: Iss. 3, Article 19.
DOI: https://doi.org/10.21123/2411-7986.5238

BAGHDAD SCIENCE JOURNAL 2026;23(3):964–975

Scan the QR to view the full-text article on the journal website

RESEARCH ARTICLE

A Novel Graphene Nanoplatelets Electrochemical Aptamer Biosensor for Glycated Human Albumin Detections

Hadi Al-Sagur [1,4,*], **Ali Al-Jawdah** [2], **Ali Al-Khazraji** [3], **Alexei Nabok** [4]

[1] Department of Physiology and Medical Physics, College of Medicine, University of Thi-Qar, Nasiriyah, Iraq
[2] Department of Physics, College of Science, University of Babylon, Hilla, Iraq
[3] General Directorate of Education in Salah Al-Din, Ministry of Education, Iraq
[4] Materials and Engineering Research Institute, Sheffield Hallam University, Sheffield, United Kingdom

ABSTRACT

This study presents the development of electrochemical biosensors for the glycated albumin (GA) sensitive detection as a crucial biomarker for monitoring glycaemic control in diabetes mellitus (DM). A ferrocene-labelled DNA aptamer specific to glycated albumin was developed as an electrochemical aptamer-based sensor to detect GA. The amine-functionalized graphene nanoplatelets (GNPs), with their enhanced surface area, provided an optimal substrate for aptamer immobilization through covalent interactions. The layer-by-layer full EDC/NHS-GNPs-Aptamer biosensor, tested by cyclic voltammetry (CV), exhibited strong redox peaks due to the good electron transfer activity between the biosensing structures. The GA-aptamer binding was studied using square wave voltammetry (SWV), and the data revealed a linear relationship for a wide range of concentrations between 10 and 10,000 μg/mL with a low limit of detection (LOD) of 0.12 μg/mL. The performance of EDC/NHS-GNPs-Aptamer-GA displayed high selectivity and good response to the low concentrations, making it a valuable tool for clinical diagnostics and the management of diabetic patients.

Keywords: Biosensor, DNA aptamer, Glycated albumin, Graphene nanoplatelets, Diabetes mellitus

Introduction

Human serum albumin (HSA) is the most abundant protein in plasma; it is synthesized primarily in the liver and excreted into the bloodstream. [1,2] Albumin composes 50% to 60% of blood plasma proteins, and its normal concentration of albumin is 35–50 grams per liter or 35 to 50 mg/mL. [3,4] This abundance associated with its structure at binding with the endo- and exo- genos compounds, such as fatty acids, vitamins, hormones, toxins, metal ions, drugs, and metabolites, allows HSA to function effectively as a transport vehicle. [5] However, elevated blood glucose concentration in patients with diabetes can lead to glycation. Glycation is a severe non-enzymatic reaction that produces glycated human serum albumin (GHSA), and it refers to the process by which glucose molecules bind to proteins in the body, forming abnormal compounds known as advanced glycation end-products (AGEs). [6] Measuring glycated hemoglobin (HbA1c) and glycated albumin is important to monitoring glycaemic control and assessing the risk of diabetic complications in individuals; however, GA exhibits a short half-life, typically ranging from 14 to 21 days, compared to HbA1c (approximately 2 to 3 months). [7] This means that GA reflects changes in blood glucose levels, providing an immediate indication of glycaemic control, and

Received 11 August 2025; revised 20 September 2025; accepted 20 October 2025.
Available online 23 March 2026

* Corresponding author.
E-mail addresses: hadi@utq.edu.iq (H. Al-Sagur), aalimadlol@yahoo.com (A. Al-Jawdah), ali.chemistry86@gmail.com (A. Al-Khazraji), alexei.nabok@gmail.com (A. Nabok).

https://doi.org/10.21123/2411-7986.5238

therefore GA could be considered as a DM marker. The normal concentration of glycated albumin (GA) in healthy individuals is approximately 11% to 16% of the concentration of the albumin in blood plasma, and this is equivalent to 2.0 – 2.85 mg/mL.[8] Several methods have been developed to detect GA level in blood, including thio-barbituric acid colorimetry,[9] boronate affinity chromatography,[10] nitro-blue tetrazolium colorimetric,[11] immunoassays,[12] enzymatic method[13] etc. These methods are all centralised laboratory-based tests; therefore, developing a simple and rapid method for measuring GA, suitable for point-of-care testing (POCT), is essential to support its application in glycaemic management.

The aptamer-based sensors offer significant advantages in comparison to traditional methods of GA detection. Aptamers are short, laboratory-engineered strands of single-stranded DNA (ssDNA) or RNA oligonucleotides designed to bind specifically to target molecules.[14,15] Typically, aptamers are acquired by repetitively isolating binders based on their affinity, then amplifying them through polymerase chain reaction (PCR) from extensive collections of random oligonucleotides. This is an *in vitro* evolution process and was first introduced in 1990 by Tuerk and Gold, who called it systematic evolution of ligands by exponential enrichment (SELEX).[16] Recently, numerous aptamers have been developed to target a variety of molecules, including proteins,[17] peptides,[18] amino acids,[19] drugs,[20] microorganisms,[21] and metal ions.[22] Among these advancements, the synthesis of aptamers for the detection of glycated albumin has gained significant interest over the past two decades.[23,24] Electrochemical methods serve as a transduction process to detect affinity and monitor electron transfer activity for aptamer biosensors.[25]

Electrochemical DNA aptamer sensors for GHSA management have been studied, though not widely, over the past decade.[26] These sensors have proven to be simple, fast, and inexpensive while also exhibiting high selectivity and sensitivity. A significant advantage of DNA aptamers comes from their high affinity and specificity to bind any biomolecular target, in addition to their easy synthesis and labelling. Various electrochemical techniques have been employed for the quantitative analysis of clinical samples. SWV is among the most rapid and highly sensitive techniques in pulse voltammetry.[27]

Electrochemical impedance spectroscopy (EIS) has been widely used to provide significant insights into the inner and outer interfaces of biosensing platforms.[28] EIS has demonstrated its ability to quantify GA bound to single-cysteine dihydrofolate reductase in synthetic urine.[29] Moreover, it was applied to study the charge transfer resistance of the electrochemical reaction at the electrodes functionalized with graphene oxide and gold nanoparticles in contact with serum. The binding of GA to the aptamer on the surface of the decorated electrode increases the interfacial resistance to electron flow.[23] The electrochemical methods of SWV, EIS, and cyclic voltammetry (CV) were extensively used as electroanalytical techniques for assessing the kinetics of electrochemical reactions with proteins at the electrode surface.[30,31] These methods have also been used to study the protein-to-aptamer binding through the modulation in the electron transfer between electrodes and a redox probe.[32] Few electrochemical transduction methods have been employed to monitor HSA.[26,33,34] Nevertheless, EIS transducers have been reported in the literature.[17,23,28] However, there remains room for further research in this area, particularly in applying nanomaterial-based platforms.

The incorporation of nanomaterials and signal amplification strategies further enhances the sensitivity and performance of the aptamer sensors, making them promising tools for clinical diagnostics and monitoring of diabetic patients.[35] Graphene nanoplatelets (GNPs) with their exceptional electrical, mechanical, and chemical properties have revolutionized sensor development. An ongoing researcher is focused on understanding the long-term impact of GNPs in biological systems to guarantee their safe implementation in sectors including drug delivery and biomedical devices.[36,37]

Herein, the core purpose of this article is to utilize GNPs to develop a novel glycated albumin sensor for medical applications. As the field advances rapidly, GNPs have demonstrated a key impact in boosting the efficiency of aptamer-based biosensors. Our method relies on the use of a screen-printed carbon electrode (SPCE) coated with EDC/NHS-GNPs as a matrix for the biomolecules' hosts.[38–40] Although many studies have been carried out using amine functionalization of graphene derivatives as a mediator in aptamer sensor studies for the detection of GA, the use of graphene nanoplatelets as the structure we established, EDC-NHS-GNPs-Aptamer-GA platform, has not yet been reported. Aptamer was immobilized and tested for GA detection, and the results exhibited a strong clinical potential of our electrochemical biosensors.

Materials and methods

Reagents and materials

Graphene nanoplatelets (GNPs) with a surface area of 500 m^2/g and sheet resistance of 10 ($\pm$5) Ω/sq (for a 25 μm film) were purchased from Sigma Aldrich (UK). GNPs contained 5–7 atomic sheets separated by anionic surfactant. Glycated human albumin (GHA)

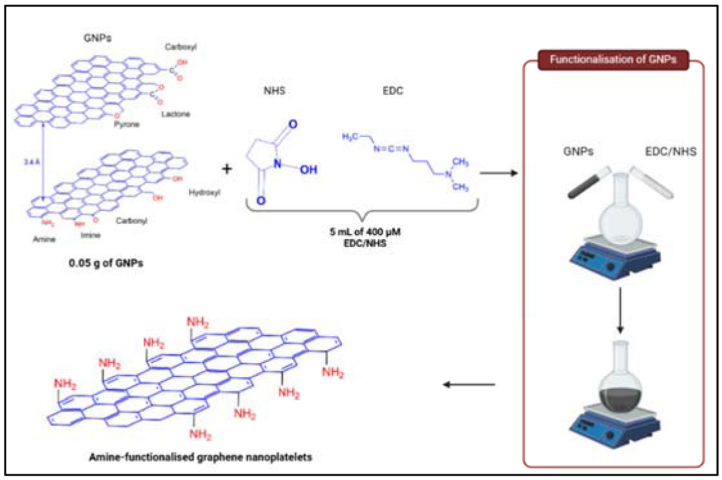

Fig. 1. Functionalization of graphene nanoplatelets to amino groups.

lyophilized powder, 1-(3-dimethylaminopropyl)-3-ethylcarbodiimide hydrochloride 98+% (EDC hydrochloride), N-Hydroxysuccinimide (NHS), phosphate buffer solution (PBS, sodium chloride (NaCl), pH 7.4), hydrochloric acid (HCl, 37% solution) were supplied by Sigma Aldrich (UK) and used as received. Tris-EDTA (TE) buffer (1X Solution pH 8.0). Low EDTA was used for reconstitution purposes of the Aptamer. Potassium ferrocyanide trihydrate 99+%, potassium ferricyanide 98%, Ethanolamine 99%, potassium chloride (KCl), and sodium chloride (NaCl) were obtained from Fisher Scientific.

Functionalization of GNPs

Functionalization of GNPs was performed by suspending 0.05g of GNPs powder in 5 mL deionized water, followed by sonication for 10 minutes to promote exfoliation of the graphene flakes.[41] The suspension was mixed with 5 mL of 400 μM EDC/NHS. The resulting mixture was stirred at room temperature for 4 hours and subsequently sonicated for an additional 10 minutes, resulting in EDC/NHS-activated graphene nanoplatelets (EDC/NHS-GNPs). The EDC/NHS-GNPs suspension was then centrifuged at 11,000 rpm for 20 minutes and washed three times with DI water to eliminate any unreacted EDC or NHS. The supernatant was removed, and the residue was dried in an oven at 30 ˚C for 24 hours. This solid form of the activated GNPs was resuspended in deionized water by stirring for 40 min. A homogeneous suspension of EDC/NHS-GNPs was achieved after approximately 10 minutes of sonication. Fig. 1 illustrates the process of functionalization of GNPs.

The functionalized GNPs were deposited on the working electrode of a SPCE by applying 7 μL of EDC/NHS-GNPs, then kept in an oven at 40 ˚C for 15 minutes to dry. Afterwards, it was gently rinsed with PBS to eliminate any unbound GNPs.

Aptamer preparation and selection

A DNA-based aptamer specific to Glycated Albumin, having 23 nucleotides with the sequence of 5'-NH2-TGCGGTTGTAGTACTCGTGGCCG-Fc-3' and functionalized with amine at the 5' terminal (Amine-Aptamer-Ferrocene) was purchased from Sangon Biotech Ltd., Shanghai, China (SI-1). The aptamer was requested from Sangon Biotech to be designed based on a procedure reported in a previous study[24] which was originally modified from the previous reports.[42] Apiwat et al. employed a modified SELEX method to repeatedly select and refine high-affinity single-stranded (ss) DNA aptamers from a large library with random sequences. Through rounds of insertion and deletion mutations using PCR amplification, selected DNA aptamers specifically bound glycated human serum albumin (GHSA), 5'TGCGGTTGTAGTACTCGTGGCCG3' has been achieved.

Immobilization of the aptamer on the EDC/NHS-GNPs sensor

This step involves first the reconstitution of the aptamer according to Sangon Biotech protocol. The aptamer was received as a lyophilized powder and diluted in Tris-EDTA buffer, where 88 μL buffer was added to make a 100 μM stock solution.

The proposed electrochemical aptamer sensor is represented step by step in the flow diagram shown in Fig. 2, illustrating the electrochemical reactions on the modified electrodes. Fig. 2 explains the binding

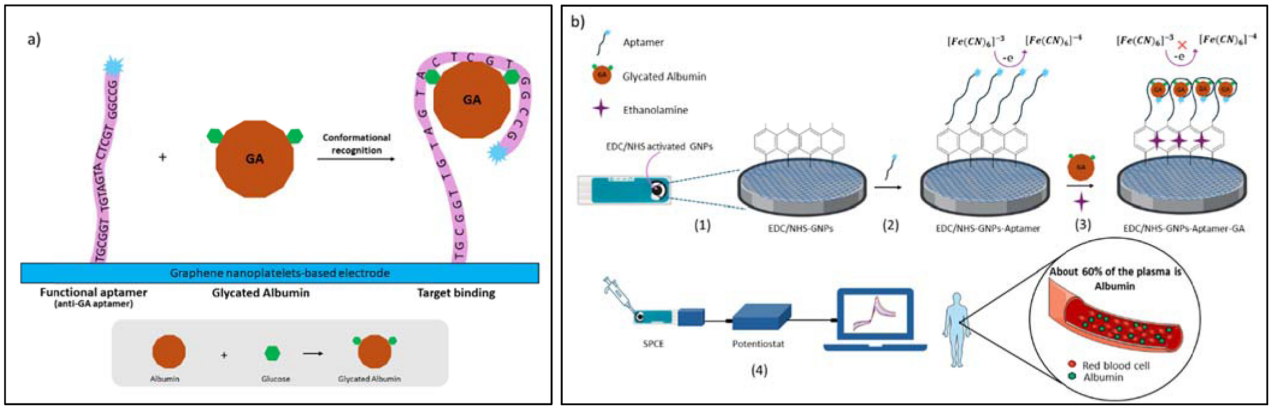

Fig. 2. a) Schematic of aptamer binding to glycated albumin. b) A flow diagram illustrates (1) the functionalization of GNPs on SPCEs; (2) the immobilization of the NH2 aptamer; (3) incubation with GA; and (4) setup for the square wave voltammetry measurements.

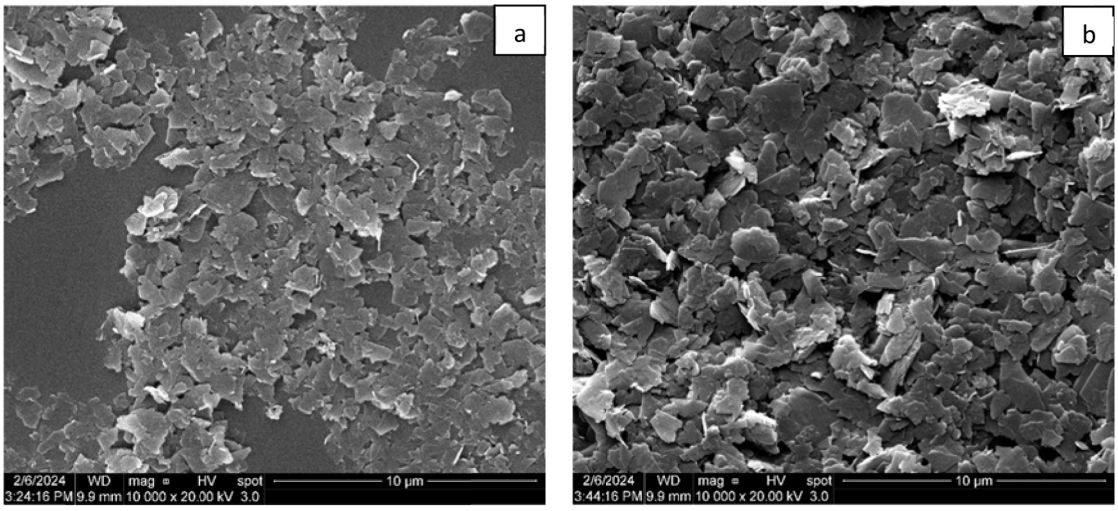

Fig. 3. SEM images of (a) pristine GNPs and (b) GNPs functionalized using EDC/NHS coupling chemistry.

interaction and how the aptamer binds to the target protein (GA), while Fig. 2 presents the overall flow diagram of the proposed sensor.

Two different procedures were carried out to immobilize the Aptamer: First, to apply 7 μL of aptamer (1 μM) to the EDC/NHS-GNPs sensor and keep it to stabilize for 35 min for complete binding between the amine-modified aptamer and carboxyl groups of the GNPs. The unbound aptamers were washed thoroughly with PBS (1×, pH 7.0). Ethanolamine 0.1 M was used as a blocking reagent to reduce non-specific binding on the surface. After blocking for 15 min, the SPCEs were washed with PBS again. This biosensor, EDC/NHS-GNPs-Aptamer, was prepared to study the confirmation of deposition via CV and EIS measurements.

The second procedure involved diluting GA in PBS (pH 7.4) to prepare different concentrations from 10 to 10,000 μg/mL of GA to be incubated with the aptamer (1 μM) for 35 min to reach the GA binding aptamer.[29] 7 μL of this mixture, Aptamer-GA applied on the EDC/NHS-GNPs sensor to produce EDC/NHS-GNPs-Aptamer-GA as a full biosensor in different concentrations of the GA to be used for SWV measurements. Thus, this is a simple two-layer system formed by successive drop-casting to fabricate the aptamer sensors of this study.

Results and discussion

Morphology of the GNPs coating

The SEM images of GNPs, Fig. 3 (a), show that the pristine GNPs appear as a smooth and flat surface. A low magnification image shows that flakes are wrinkled and spread homogeneously on the surface. The GNPs functionalized with EDC/NHS have exhibited flat, sheet-like layers, with noticeable differences in surface texture compared to untreated GNPs. The feature is faintly lighter spots or irregularities due to the attachment of carboxyl or amine groups Fig. 3 (b). Functionalization with EDC/NHS is often done

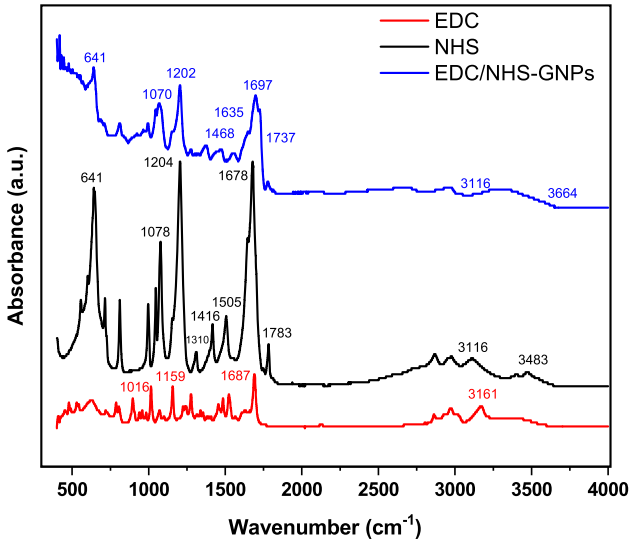

Fig. 4. FT-IR spectra of EDC and NHS crosslinkers and the functionalized GNPs.

to enable further binding with biomolecules or other compounds, so the resulting GNPs would have a more reactive surface, useful for biomedical or sensor applications. GNPs functionalized with EDC/NHS illustrate a homogeneous and smooth texture. The smooth or slightly wrinkled GNP sheets may now display faintly lighter spots or irregularities due to the attachment of carboxyl or amine groups.

FT-IR characterization was performed to confirm the functionalization of GNPs to the cross-linker EDC/NHS. The FTIR spectra of the functionalized GNPs and the crosslinkers GNPs-EDC/NHS, EDC, and NHS are shown in Fig. 4. The absorption spectra of GNPs-EDC/NHS have exhibited stretching vibration of hydroxyl groups -OH at 3664 to 3116 cm^{-1}, carbonyl groups 1737 to 1697 cm^{-1} that inherent features of graphene, carboxyl groups 1635 cm^{-1}, the presence of C-OH at 1468 cm^{-1}, and amine groups N-H at 1635 to 1468 cm^{-1}.[43] The absence of characteristic peaks in the GNPs powder suggests a free-oxygen structure, confirming its hydrophilic nature.[44] The NHS presented two remarkable peaks: one at 1678 cm^{-1} corresponding to N–O, and 1783 cm^{-1} attributed to C=O bonds.[45,46] Typical peaks of EDC have appeared at 1687 cm^{-1} represent amide group peak I, 1500 cm^{-1} C=N stretching, 1016 cm^{-1} to the CH2 bending, and 1159 cm^{-1}.[47]

Electrochemical characterization of the aptamer sensor

Cyclic voltammetry was utilised to confirm the successful deposition of each biomolecular layer of the biosensor, where noticeable electrochemical changes observed at each modification stage as shown in Fig. 5. Cyclic voltammograms of bare, pristine GNPs, EDC/NHS, EDC/NHS-GNPs modified electrodes in addition to the EDC/NHS-GNPs-Aptamer and incubated biosensors were all recorded in a solution of 5 mM of potassium ferro/ferricyanide $[Fe(CN)_6]^{-3/-4}$ and containing 0.1 M NaCl. The ferricyanide $[Fe(CN)_6]^{-3}$ utilises as an electron acceptor and is reduced to ferrocyanide $[Fe(CN)_6]^{-4}$ and the generated electrons flow between the working electrode surface and the bulk solution.[48] The couple redox acts as a benchmark system within a potential range from $+1$ to -1 V at a scan rate of 0.05 Vs^{-1}, as illustrated in Fig. 5. Well-defined reversible peaks associated with the Fe(II)/Fe(III) redox transition were observed in the CVs of the biosensor developed on the platform. The efficiency of the platforms was evaluated via identify the potentials of the cathodic (E_{pc}) and anodic (E_{pa}) peaks, as well as the peak separation ($\Delta E_p = E_{pa} - E_{pc}$).

GNPs-modified SPCE (green curve) exhibited a higher peak current than bare SPCE (brown curve). A significant shift in the anodic (E_{pa}) and cathodic (E_{pc}) potentials resulted in a reduced peak-to-peak separation (ΔE_p). ΔE_p was 0.20 V in the presence of GNPs, while 0.16 V at the bare electrode, and this illustrates that GNPs have increased the electron transfer rate on the electrode surface. Moreover, there was a significant increase in both anodic (I_{pa}) and cathodic (I_{pc}) currents from 104 μA to 145 μA and -75 μA to -142 μA, respectively. This can be attributed to the enhancement in the transfer electron activity of the functionalised GPNs with EDC/NHS (red curve), as it has been previously reported in

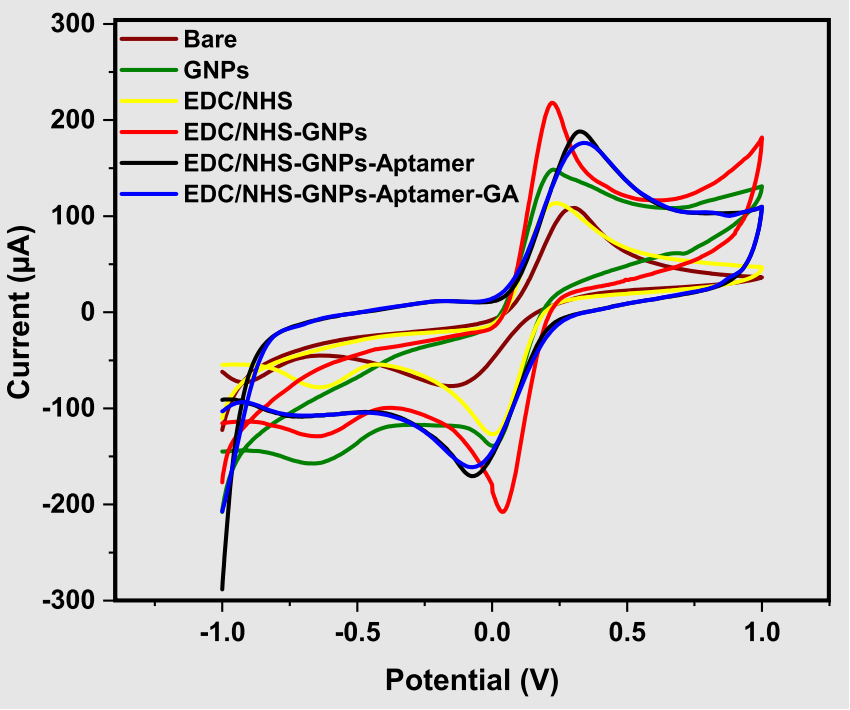

Fig. 5. Cyclic voltammetry of the fabricated platforms was tested in a solution of 5 mM potassium ferro/ferricyanide $[Fe(CN)_6]^{-3/-4}$ containing 0.1 M NaCl, as explained in the legends.

the bibliography.[49,50] This fully modified platform, EDC-NHS-GNPs, shows a dramatic increase in the cathodic and anodic current to the redox peak, also due to the stable functionalisation of the GNPs. On the other hand, the EDC/NHS sensor (yellow curve) was scanned and exhibited similar intensity to the bare sensor due to the lack of any electrocatalytic elements on the surface of the sensor, which confirms how GNPs enhance the charge transfer rate on the sensor surface during the electrochemical reactions.

The fully assembled biosensor, following aptamer immobilization (EDC/NHS-GNPs-Aptamer, black curve), showed a decline in the redox peak intensity, which was attributed to the aptamer's large structure and its negative charge. The peak decreased further following target incubation, attributed to a conformational change in the aptamer upon specific protein binding, EDC/NHS-GNPs-Aptamer-GA (blue curve). The GA-Aptamer complex acted as a blocking layer on the sensor surface, which obstructed the electron transfer activity during the reaction. Further decrease in the CV current took place after testing the incubated Aptamer-GA due to hindering the diffusion of electrons from the redox probe reaction to the surface of the electrode, which not only confirms the correct binding of the aptamer on the sensor surface but also demonstrates that it retains its recognition ability.

The electrochemical affinity of the aptamer to GA

The EIS measurements of the electrochemical biosensor have been carried out to examine the binding affinity between the aptamer and GA. The EIS of bare, GNPs, EDC/NHS-GNPs, and EDC/NHS-GNPs-Aptamer biosensor was tested in a solution of 5 mM $[Fe(CN)_6]^{-3/-4}$ including 0.1 M NaCl, and the results are shown in Fig. 6.

The Nyquist plot for the bare SPCEs exhibited a small semicircular diameter, which refers to a smaller charge-transfer resistance at the electrode and indicates a high level of electron transfer rate between the redox solution $[Fe(CN)_6]^{-3/-4}$ and the electrode surface. The increase in Z" at low frequencies is associated with the limitation of diffusion of redox groups to the electrode surface. EDC/NHS-GNPs-aptamer biosensor has exhibited higher values of R_{ct}, which confirms the immobilisation of aptamers, which reduces charge transfer at the electrode. The binding of large GA proteins to aptamers caused further blockage[34] or hindering[17] of charge transfer and thus even larger values of R_{ct}, which confirmed the affinity of the aptamer under study to the GA.

In addition to studying the characteristics of the electrochemical interfaces on the functionalized electrodes, further analysis of EIS spectra was perfumed by applying data fitting to the Randle's model

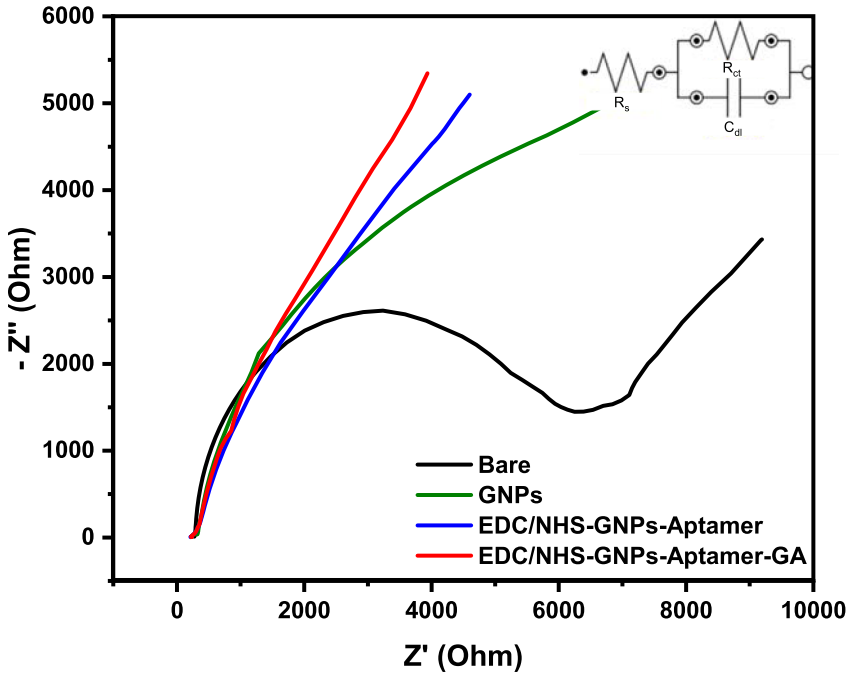

Fig. 6. EIS of the fabricated platforms was tested in a solution of 5 mM potassium ferro/ferricyanide $[Fe(CN)_6]^{-3/-4}$ including 0.1 M NaCl, as explained in the legends.

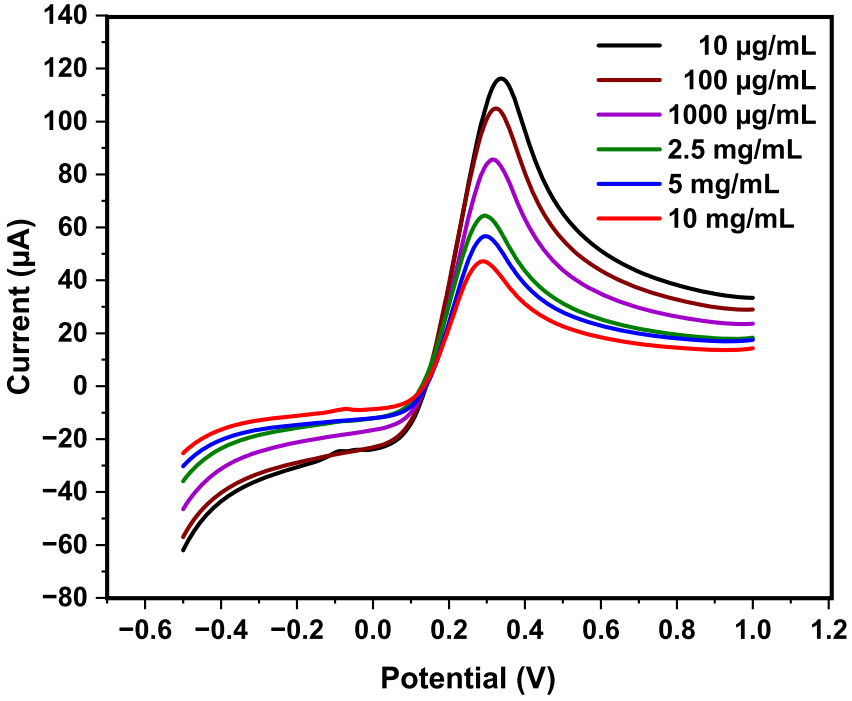

Fig. 7. Typical SWV responses of EDC/NHS-GNPs-Aptamer samples after incubation with 10 μg/mL (black), 100 μg/mL (brown), 1000 μg/mL (purple), 2.5 mg/mL (green), 5 mg/mL (blue), and 10 mg/mL (red) of GA.

equivalent circuit model ($R_s(R_{ct}C_{dl})$ (inset of Fig. 6) was carried out with Dropview 8400 software and demonstrated good agreement between the simulated and experimental data within the frequency range of 10 Hz – 2 MHz. The results show that solution resistance (R_s) is 302.91 Ω , charge transfer resistance (R_{ct}) is 7480.8 Ω, and the double-layer capacitance (C_{dl}) is 60.608 μF.

Analytical performance of the electrochemical aptamer sensor

The fabricated sensors were evaluated in GA solutions at concentrations ranging from 10 μg/mL to 10 mg/mL. After incubating the electrodes in GA solutions for 40 min, the SWV measurements were carried out. A typical series of SWV curves shown in Fig. 7 demonstrates the decrease in the peak current with increasing GA concentrations. The association between the peak current and GA levels confirmed that the formation of the GA-Aptamer complex acts as a blocking layer on the sensor surface, thereby decreasing charge transfer.

The variations in the SWV peak current in relation to the natural logarithm of GA concentrations over a range between 10 and 10,000 μg/mL displayed in Fig. 8 were described by the following linear regression in Eq. (1).[17]

$$\Delta I\ (\mu A) = a \ln C\ (\mu g/mL) + b \quad (1)$$

Where, $\Delta I\ (\mu A) = 0.1413 \ln C\ (\mu g/mL) + 0.1579$ and $R^2 = 0.9858$.

LOD was established by applying the formula LOD $= 3\sigma/S$ with σ representing the standard deviation of SWV signals at minimal GA concentrations, and S signifies the slope of the linear calibration curve, shown below in Fig. 8. The calculated LOD was 0.12 μg/mL, representing the minimum GA concentration that can be consistently detected. This result highlights the high sensitivity of the aptamer-based biosensor.

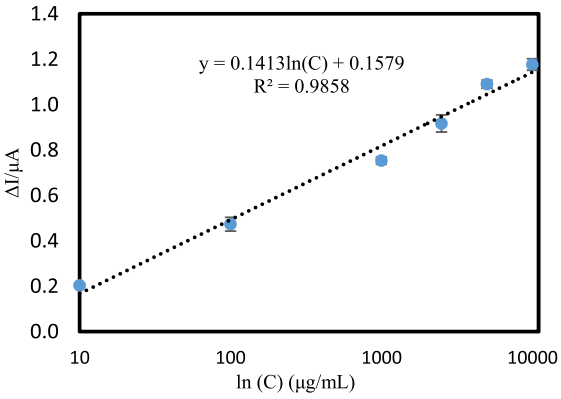

Fig. 8. Calibration plot showing the linear core between the SWV peaks (ΔI) and the natural logarithm of GA concentrations (ln C).

Table 1 provides a comparison of the performance of previously reported biosensors for GA detection with that of our graphene nanoplatelets probe. Results reveal that the prepared GNPs-based probe exhibited good performance and accuracy for the detection of GA macromolecules, which is clinically relevant to normal ranges 2.0 – 2.85 mg/mL. Reproducibility, repeatability, and stability have been studied for the sensor. For reproducibility, ten independent electrodes of EDC/NHS–GNPs-Aptamer-GA were fabricated under the same conditions. Their SWV current responses were consistent, with relative standard deviation (RSD) values of ≈1.27%. One electrode of EDC/NHS–GNPs-Aptamer-GA was tested seven times, with two repeats each time. The RSD obtained was ≈ 1.34 %, confirming good repeatability. Aptamer–GA modified biosensors stored at 4 ˚C retained 98% of their initial signal after 24 h demonstrate the stability of our biosensor. The designed sensor is intended as a single-use device. A selectivity test was conducted to evaluate the interactions of common plasma biomolecules with the Aptamer-GA sensor. Each compound (GA, glucose, ascorbic acid, ampicillin, and folic acid) was individually tested at a concentration of 2.5 mg/mL in the presence of redox probe solution using SWV measurements to assess potential interference. The sensor's response, defined as the SWV oxidation peak current, demonstrated high specificity towards the GA, as illustrated in Fig. 9. This result is consistent with previous studies that have also reported high specificity towards the same target.[17,24,26] The accuracy of the sensor was calculated using Eq. (2), yielding a value of 98.3% based on the relative error between the measured and true value.[12]

$$Accuracy\ (\%) = 1 - \left(\frac{|Measured - True|}{True}\right) \times 100 \quad (2)$$

Table 1. LOD of different aptamer sensors for identifying glycated albumin.

Detection method	Target	Platform	LOD	Measurement range	Reference
SPCE	GA	STR-Aptamer-GHSA	0.003 μg/mL	0.002–16 mg/mL	48
SPCE	GA	EDC-NHS-GO	0.031 μg/mL	0.001–10 mg/mL	17
SPCE	GA	Au Nis/Aptamer		1–40 mg/mL	26
SPCE	GA	AgNP/PPA & AuNP/PPA		10 to 400 μg/mL	33
Glassy carbon electrode	GA	GCE/RGO/AUNPs/Apt-GA	0.07 μg/mL	8 – 36 mg/mL	23
SPCE	GA	EDC/NHS-GNPs-Aptamer-GA	0.12 μg/mL	10–10,000 μg/mL	This work

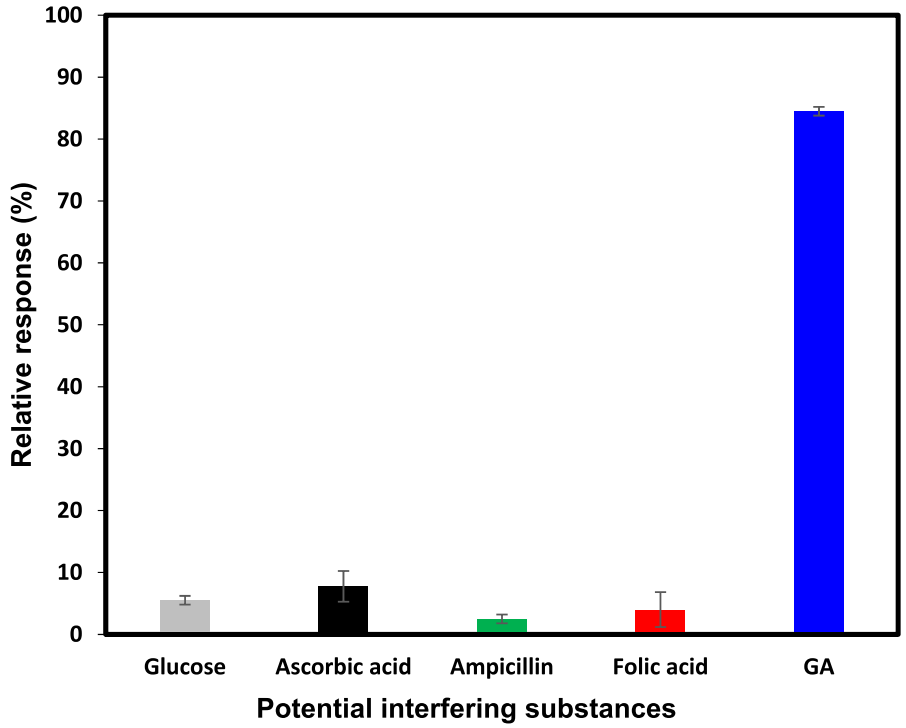

Fig. 9. Selectivity of EDC/NHS-GNPs-Aptamer-GA sensor toward 2.5 mg/mL GA compared with potential interfering substances (ampicillin, ascorbic acid, glucose, and folic acid), measured in PBS containing 5 mM potassium ferro/ferricyanide solution $[Fe(CN)_6]^{-3/-4}$.

The relative response (%) was calculated based on the SWV oxidation peak current using the formula in Eq. (3).

$$Relative\ response\ (\%) = \left(\frac{I_{analyte}}{I_{GA}}\right) \times 100 \qquad (3)$$

Where $I_{analyte}$ is the current response of the interfering species and I_{GA} is the response to GA. Results indicate high selectivity toward GA.

Conclusion

The primary result of the study is a demonstration of a simple electrochemical aptamer sensor for GA detection, which benefited from the high dispersibility of GNPs as an efficient host matrix for aptamer immobilization. Our developed biosensor performed effectively over an extensive range of concentrations from 10 to 10,000 μg/mL, where it demonstrated a low LOD of 0.12 μg/mL, which is sufficient for medical analysis. In addition, CV, EIS, and selectivity analysis confirmed the strong analytical performance of the biosensor. The biosensor exhibited excellent selectivity, reproducibility, repeatability, and long-term stability indicating strong and well-engineered interactions among the platform's components. Furthermore, the sensor demonstrated high accuracy, yielding a value of 98.3%. The developed aptamer sensor provides great synergy between aptamers and graphene nanoplatelets in biosensing applications and shows their combined potential in numerous applications such as medical diagnostics, environmental monitoring, and biomedical research. The possible practical application of our device could be in point-of-care testing of GA levels for the monitoring of diabetes mellitus.

Acknowledgment

Dr. Hadi Al-Sagur expresses gratitude to the College of Medicine at the University of Thi-Qar, Iraq, and the Materials and Engineering Research Institute (MERI), Sheffield Hallam University, UK, for their invaluable technical assistance throughout the course of this research. This study was entirely self-funded by Mr. Al-Sagur with no external financial contributions.

Authors' declaration

- Conflicts of Interest: None.
- We hereby confirm that all the Figures and Tables in the manuscript are ours. Furthermore, any Figures and images that are not ours have been included with the necessary permission for republication, which is attached to the manuscript.
- No animal studies are present in the manuscript.

- No human studies are present in the manuscript.
- Ethical Clearance: The project was approved by the local ethical committee at Sheffield Hallam University.

Authors' contribution statement

H.A. and A.N. designed the study. H.A. wrote the first draft of the manuscript, performed the methodology, analyzed the data, carried out the calculations, designed schemes and figures, and wrote the entire discussion.

A.N., A.Al-J. and A. Al-K. conducted the final review and provided critical revisions.

References

1. Qiu HY, Hou NN, Shi JF, Liu YP, Kan CX, Han F, *et al.* Comprehensive overview of human serum albumin glycation in diabetes mellitus. World J Diabetes. 2021 Jul 15;12(7):1057–69. https://doi.org/10.4239/wjd.v12.i7.1057.
2. Rothschild MA, Oratz M, Schreiber SS. Serum albumin. Hepatology. 1988;8(2):385–401. https://doi.org/10.1002/hep.1840080234.
3. Arasteh A, Farahi S, Habibi-Rezaei M, Moosavi-Movahedi AA. Glycated albumin: An overview of the In Vitro models of an In Vivo potential disease marker. Journal of Diabetes & Metabolic Disorders. 2014;13:49. https://doi.org/10.1186/2251-6581-13-49.
4. Evans T. W. Albumin as a drug: its biological effects of albumin unrelated to. Aliment Pharmacol Ther. 2002; 16(suppl 5):6–11. https://doi.org/10.1046/j.1365-2036.16.s5.2.x.
5. Szkudlarek A, Pożycka J, Kulig K, Owczarzy A, Rogóż W, Maciążek-Jurczyk M. Changes in Glycated Human Serum Albumin Binding Affinity for Losartan in the Presence of Fatty Acids In Vitro Spectroscopic Analysis. Molecules. 2022 Jan 1;27(2). https://doi.org/10.3390/molecules27020401.
6. Anguizola J, Matsuda R, Barnaby OS, Hoy KS, Wa C, DeBolt E. Review: Glycation of human serum albumin. Clin Chim Acta. 2013 Oct 21;425:64–76. https://doi.org/10.1016/j.cca.2013.07.013.
7. Ibrahim R khuldon, Ghudhaib KK, Allawi AAD. ATPase level in Iraqi Diabetic Patients with and without Diabetic Kidney Disease. Baghdad Sci. J. 2025 Jun 17;22(6):1750–6. https://doi.org/10.21123/2411-7986.4952.
8. Ciaccio M. Introduction of glycated albumin in clinical practice. J Lab Precis Med. 2019;4:28. https://doi.org/10.21037/jlpm.2019.08.02.
9. Rendell M, Kao G, Mecherikunnel P, Petersen B, Duhaney R, Nierenberg J, *et al.* Aminophenylboronic acid affinity chromatography and thiobarbituric acid colorimetry compared formeasuring glycated albumin. Clin Chem. 1985;229–34. https://doi.org/10.1093/clinchem/31.2.229.
10. Silver AC, Lamb E, Cattell WR, Dawnay AB. Investigation and validation of the affinity chromatography method for measuring glycated albumin in serum and urine. Clin Chim Acta. 1991 Oct 14;202(1-2):11–22. https://doi.org/10.1016/0009-8981(91)90251-7.
11. Mashiba S, Uchida K, Okuda S, Tomita S. Measurement of glycated albumin by the nitroblue tetrazolium colorimetric method. Clin Chim Acta. 1992 Nov 16;212(1–2):3–15. https://doi.org/10.1016/0009-8981(92)90133-B.
12. Choi H, Son SE, Hur W, Tran VK, Lee HBB, Park Y, *et al.* Electrochemical Immunoassay for Determination of Glycated Albumin using Nanozymes. Sci Rep. 2020 Dec 1;10(1). https://doi.org/10.1038/s41598020664463.
13. Chume FC, Correa Freitas PA, Schiavenin LG, Sgarioni E, Leitao CB, Camargo JL. Glycated albumin in the detection of diabetes during COVID-19 hospitalization. PLoS One. 2024 Mar;19(3):e0297952. https://doi.org/10.1371/journal.pone.0297952.
14. Cech TR. A model for the RNA-catalyzed replication of RNAt Proc Natl Acad Sci. 1986 Jun;83(12):4360–3. https://doi.org/10.1073/pnas.83.12.4360.
15. Ellington A, Szostak J. In vitro selection of RNA molecules that bind specific ligands. Nature. 1990 Aug 30;346(6287):818–22. https://doi.org/10.1038/346818a0.
16. Tuerk C, Gold L. Systematic evolution of ligands by exponential enrichment: RNA ligands to bacteriophage T4 DNA polymerase. Science. 1990 Aug 3;249(4968):505–10. https://doi.org/10.1126/science.2200121.
17. Aye NN, Maraming P, Tavichakorntrakool R, Chaibunruang A, Boonsiri P, Daduang S, Teawtrakul N, *et al.* A simple graphene functionalized electrochemical aptasensor for the sensitive and selective detection of glycated albumin. Appl Sci. 2021 Nov 3;11(21):10315. https://doi.org/10.3390/app112110315.
18. He XY, Ren XH, Peng Y, Zhang JP, Ai SL, Liu BY, *et al.* Aptamer/peptide-functionalized genome-editing system for effective immune restoration through reversal of PD-L1-mediated cancer immunosuppression. Advanced materials. 2020 Apr;32(17):2000208. https://doi.org/10.1002/adma.201906425.
19. Mannironi C, Scerch C, Fruscoloni P, Tocchini-Valentini GP. Molecular recognition of amino acids by RNA aptamers: The evolution into an L-tyrosine binder of a dopamine-binding RNA motif. Rna. 2000 Apr;6(4):520–7. https://doi.org/10.1017/S135583820000057X.
20. Xie M, Zhao F, Zhang Y, Xiong Y, Han S. Recent advances in aptamer-based optical and electrochemical biosensors for detection of pesticides and veterinary drugs. Food Control. 2022 Jan 1;131:108399. https://doi.org/10.1016/j.foodcont.2021.108399.
21. Chung J, Kang JS, Jurng JS, Jung JH, Kim BC. Fast and continuous microorganism detection using aptamer-conjugated fluorescent nanoparticles on an optofluidic platform. Biosens Bioelectron. 2015 May 5;67:303–8. https://doi.org/10.1016/j.bios.2014.08.039.
22. Srinivasan S, Ranganathan V, McConnell EM, Murari BM, DeRosa MC. Aptamer-based colorimetric and lateral flow assay approaches for the detection of toxic metal ions, thallium(i) and lead(ii). RSC Adv. 2023 Jul 4;13(29):20040–9. https://doi.org/10.1039/D3RA01658G.
23. Farzadfard A, Shayeh JS, Habibi-Rezaei M, Omidi M. Modification of reduced graphene/Au-aptamer to develop an electrochemical based aptasensor for measurement of glycated albumin. Talanta. 2020 May 1;211. https://doi.org/10.1016/j.talanta.2020.120722.
24. Apiwat C, Luksirikul P, Kankla P, Pongprayoon P, Treerattrakoon K, Paiboonsukwong K, *et al.* Graphene based aptasensor for glycated albumin in diabetes mellitus diagnosis and monitoring. Biosens Bioelectron. 2016 Aug 15;82:140–5. https://doi.org/10.1016/j.bios.2016.04.039.
25. Ben Aissa S, Cass AEG. Systematic optimisation of an integrated electrochemical aptamer-based sensor for cortisol detection. Sens Actuators B Chem. 2025 Dec 1;444. https://doi.org/10.1016/j.snb.2023.114704.

26. Ghosh Dastidar M, Murugappan K, R. Nisbet D, Tricoli A. Simultaneous electrochemical detection of glycated and human serum albumin for diabetes management. Biosens Bioelectron. 2024 Feb 15;246. https://doi.org/10.1016/j.bios.2023.114542.
27. Megale JD, De Souza D. New approaches in antibiotics detection: The use of square wave voltammetry. J Pharm Biomed Anal. 2023 Sep 20;234:115526. https://doi.org/10.1016/j.jpba.2023.115276.
28. Bunyarataphan S, Dharakul T, Fucharoen S, Paiboonsukwong K, Japrung D. Glycated Albumin Measurement Using an Electrochemical Aptasensor for Screening and Monitoring of Diabetes Mellitus. Electroanalysis. 2019 Nov 1;31(11):2254–61. https://doi.org/10.1002/elan.201900280.
29. Hatada M, Pavlidis S, Sode K. Development of a glycated albumin sensor employing dual aptamer-based extended gate field effect transistors. Biosens Bioelectron. 2024 May 1;251. https://doi.org/10.1016/j.bios.2023.115223.
30. Sakata T, Shiratori R, Nishitani S. Aptamer-Based Glycated Albumin Sensor for Capacitive Spectroscopy. Anal Chem. 2023 Jan 17;95(2):1480–9. https://doi.org/10.1021/acs.analchem.2c04079.
31. Attar AM, Richardson MB, Speciale G, Majumdar S, Dyer RP, Sanders EC, *et al.* Electrochemical Quantification of Glycated and Non-glycated Human Serum Albumin in Synthetic Urine. ACS Appl Mater Interfaces. 2019 Feb 6;11(5):4757–65. https://doi.org/10.1021/acsami.8b20087.
32. Al-Rubaye AG, Nabok A, Catanante G, Marty JL, Takács E, Székács A. Label-free optical detection of mycotoxins using specific aptamers immobilized on gold nanostructures. Toxins (Basel). 2018 Jul 16;10(7). https://doi.org/10.3390/toxins10070291.
33. Pilz FH, Kielb P. Cyclic voltammetry, square wave voltammetry or electrochemical impedance spectroscopy? Interrogating electrochemical approaches for the determination of electron transfer rates of immobilized redox proteins. BBA advances. 2023 Jan 1;4:100095. https://doi.org/10.1016/j.bbadva.2023.100095.
34. Liu S, Xing X, Yu J, Lian W, Li J, Cui M, *et al.* A novel label-free electrochemical aptasensor based on graphene-polyaniline composite film for dopamine determination. Biosens Bioelectron. 2012 Jun;36(1):186–91. https://doi.org/10.1016/j.bios.2012.03.002.
35. Thongwattana T, Chaiyo R, Ponsanti K, Tangnorawich B, Pratumpong P, Toommee S, *et al.* Synthesis of Silver Nanoparticles and Gold Nanoparticles Used as Biosensors for the Detection of Human Serum Albumin-Diagnosed Kidney Disease. Pharmaceuticals. 2024 Nov 1;17(11). https://doi.org/10.3390/ph17111522.
36. Yoon J, Shin M, Kim D, Lim J, Kim HW, Kang T, *et al.* Bionanohybrid composed of metalloprotein/DNA/MoS_2/peptides to control the intracellular redox states of living cells and its applicability as a cell-based biomemory device. Biosens Bioelectron. 2022 Jan 15;196:113725. https://doi.org/10.1016/j.bios.2021.113725.
37. Tamaddon AM, Bashiri R, Najafi H, Mousavi K, Jafari M, Borandeh S, *et al.* Biocompatibility of graphene oxide nanosheets functionalized with various amino acids towards mesenchymal stem cells. Heliyon. 2023 Aug 1;9(8). https://doi.org/10.1016/j.heliyon.2023.e18637.
38. Dreyer DR, Park S, Bielawski CW, Ruoff RS. The chemistry of graphene oxide. Chem Soc Rev. 2010;39(1):228–40. https://doi.org/10.1039/b917103g.
39. Peña-Bahamonde J, Nguyen HN, Fanourakis SK, Rodrigues DF. Recent advances in graphene-based biosensor technology with applications in life sciences. J Nanobiotechnol. 2018 Sep 22;16(1):75. https://doi.org/10.1186/s12951-018-0390-z.
40. Fu L, Zheng Y, Li X, Liu X, Lin CT, Karimi-Maleh H. Strategies and applications of graphene and its derivatives-based electrochemical sensors in cancer diagnosis. Molecules. 2023 Sep 20;28(18):6719. https://doi.org/10.3390/molecules28186719.
41. Yeşiltaş G. Modification of graphene surfaces for detection of biomicroparticles [Master's thesis]. İzmir, Turkey: İzmir Institute of Technology; 2019.
42. Higashimoto Y, Yamagishi S ichi, Nakamura K, Matsui T, Takeuchi M, Noguchi M, *et al.* In vitro selection of DNA aptamers that block toxic effects of AGE on cultured retinal pericytes. Microvasc Res. 2007 Jul;74(1):65–9. https://doi.org/10.1016/j.mvr.2007.03.002.
43. Cai X, Jiang Z, Zhang X, Zhang X. Effects of tip sonication parameters on liquid phase exfoliation of graphite into graphene nanoplatelets. Nanoscale Res Lett. 2018 Dec;13(1):241. https://doi.org/10.1186/s11671-018-2598-7.
44. Parsamehr PS, Zahed M, Tofighy MA, Mohammadi T, Rezakazemi M. Preparation of novel cross-linked graphene oxide membrane for desalination applications using (EDC and NHS)-activated graphene oxide and PEI. Desalination. 2019 Oct 15;468. https://doi.org/10.1016/j.desal.2019.114054.
45. Al-Sagur H, Shanmuga sundaram K, Kaya EN, Durmuş M, Basova T V., Hassan A. Amperometric glucose biosensing performance of a novel graphene nanoplatelets-iron phthalocyanine incorporated conducting hydrogel. Biosens Bioelectron. 2019 Aug 15;139. https://doi.org/10.1016/j.bios.2019.111323.
46. Zu Y, Zhao Q, Zhao X, Zu S, Meng L. Process optimization for the preparation of oligomycin-loaded folate-conjugated chitosan nanoparticles as a tumor-targeted drug delivery system using a two-level factorial design method. Int J Nanomedicine. 2011;6:3429–41. https://doi.org/10.2147/IJN.S24644.
47. Mohamed R, Adnan N, Jawad H, Mohammed B, Mahdi R. Improvement of the physical properties of poly vinyl alcohol nanofibers by adding carbon nanotubes. Baghdad Sci J. 2025;22(3):955–65. https://doi.org/10.21123/bsj.2024.10653.
48. Ma X, Zhong W, Zhao J, Suib SL, Lei Y. "Self-heating" enabled one-pot synthesis of fluorescent carbon dots. Eng Sci. 2019 Jul 12;9:21–30. https://doi.org/10.30919/es8d805.
49. Al-Sagur H, Komathi S, Karakaş H, Atilla D, Gürek AG, Basova T, *et al.* A glucose biosensor based on novel Lutetium bis-phthalocyanine incorporated silica-polyaniline conducting nanobeads. Biosens Bioelectron. 2018 Apr 15;102:637–45. https://doi.org/10.1016/j.bios.2017.12.004.
50. Yang JH, Kim HR, Lee JH, Jin JH, Lee HU, Kim SW. Electrochemical properties of enzyme electrode covalently immobilized on a graphite oxide/cobalt hydroxide/chitosan composite mediator for biofuel cells. Int J Hydrogen Energy. 2021 Jan 14;46(4):3251–8. https://doi.org/10.1016/j.ijhydene.2020.11.140.

مستشعر حيوي أبتاميري كهروكيميائي مبتكر قائم على صفائح الجرافين النانوية للكشف عن ألبومين الإنسان المُسَكَّر

هادي والي صاحب الصكر[1،4]، علي مدلول جودة[2]، علي حازم الخزرجي[3]، الكسي نابوك[4]

[1] فرع الفسلجة والفيزياء الطبية، كلية الطب، جامعة ذي قار، الناصرية، العراق.
[2] قسم الفيزياء، كلية العلوم، جامعة بابل، الحلة، العراق.
[3] المديرية العامة لتربية صلاح الدين، وزارة التربية، العراق.
[4] معهد أبحاث المواد والهندسة، جامعة شفيلد هالام، شفيلد، المملكة المتحدة.

الخلاصة

تقدّم هذه الدراسة تطوير مستشعرات حيوية كيميائية كهربائية للكشف الحسّاس عن الألبومين المُسَكَّر(GA) ، بوصفه مؤشّرًا حيويًا مهمًا لمراقبة ضبط سكر الدم لدى مرضى داء السكري. تم تطوير أبتامر DNA موسوم بالفِيرُوسين ومخصَّص للألبومين المُسَكَّر، ليُستخدم كمستشعر كيميائي كهربائي قائم على الأبتامر للكشف عن GA. وفّرت صفائح الغرافين النانوية المُفعَّلة بمجموعة الأمين(GNPs) ، بفضل مساحتها السطحية العالية، ركيزةً مثالية لتثبيت الأبتامر من خلال تفاعلات تساهمية. وقد تم اختبار المستشعر الحيوي المتكامل المُحضَّر بطريقة الطبقات المتتابعة (EDC/NHS-GNPs-Aptamer) باستخدام تقنية الفولتمترية الدورية(CV) ، حيث أظهر قمم أكسدة-اختزال واضحة نتيجة كفاءة انتقال الإلكترونات بين مكوّنات البنية الحيوية الحسّاسة. كما تمت دراسة ارتباط GA بالأبتامر باستخدام فولتمترية الموجة المربعة(SWV) ، وأظهرت النتائج علاقة خطية ضمن مدى واسع من التراكيز يتراوح بين 10 و10,000 ميكروغرام/مل، مع حد كشف منخفض (LOD) بلغ 0.12 ميكروغرام/مل. وأظهر النظام (EDC/NHS-GNPs-Aptamer-GA) انتقائية عالية واستجابة جيدة عند التراكيز المنخفضة، مما يجعله أداة واعدة للتشخيص السريري وإدارة حالات مرضى السكري.

الكلمات المفتاحية: مستشعر حيوي، أبتامر DNA، الألبومين المُسَكَّر، صفائح الغرافين النانوية، داء السكري.